

Influence of lattice strain on charge/orbital ordering and phase separation in Pr_{0.7}(Ca_{0.6}Sr_{0.4})_{0.3}MnO₃ thin films

Y. Y. Zhao, J. Wang, F. X. Hu, H. Kuang, R. R. Wu, X. Q. Zheng, J. R. Sun, and B. G. Shen

Citation: *Journal of Applied Physics* **115**, 17D708 (2014); doi: 10.1063/1.4863383

View online: <http://dx.doi.org/10.1063/1.4863383>

View Table of Contents: <http://scitation.aip.org/content/aip/journal/jap/115/17?ver=pdfcov>

Published by the **AIP Publishing**

Articles you may be interested in

[Pressure dependence of resistivity and magnetoresistance in Pr-doped La_{0.7}Ca_{0.3}MnO₃](#)

J. Appl. Phys. **113**, 17D721 (2013); 10.1063/1.4800679

[Strain effect caused by substrates on phase separation and transport properties in Pr_{0.7}\(Ca_{0.8}Sr_{0.2}\)_{0.3}MnO₃ thin films](#)

J. Appl. Phys. **111**, 07D721 (2012); 10.1063/1.3678297

[Ferroelectricity-induced resistive switching in Pb\(Zr_{0.52}Ti_{0.48}\)O₃/Pr_{0.7}Ca_{0.3}MnO₃/Nb-doped SrTiO₃ epitaxial heterostructure](#)

Appl. Phys. Lett. **100**, 113505 (2012); 10.1063/1.3694016

[Influence of structural disorder on magnetic and transport properties of \(La_{0.7}Sr_{0.3}\)_{0.5}\(Pr_{0.65}Ca_{0.35}\)_{0.5}MnO₃ films](#)

Low Temp. Phys. **31**, 161 (2005); 10.1063/1.1820566

[Interface-oxygen-loss-controlled voltage offsets in epitaxial Pb\(Zr_{0.52}Ti_{0.48}\)O₃ thin-film capacitors with La_{0.7}Sr_{0.3}MnO₃ electrodes](#)

Appl. Phys. Lett. **85**, 5013 (2004); 10.1063/1.1827929



Not all AFMs are created equal
Asylum Research Cypher™ AFMs
There's no other AFM like Cypher

www.AsylumResearch.com/NoOtherAFMLikeIt

OXFORD
INSTRUMENTS
The Business of Science®

Influence of lattice strain on charge/orbital ordering and phase separation in $\text{Pr}_{0.7}(\text{Ca}_{0.6}\text{Sr}_{0.4})_{0.3}\text{MnO}_3$ thin films

Y. Y. Zhao, J. Wang,^{a)} F. X. Hu,^{a)} H. Kuang, R. R. Wu, X. Q. Zheng, J. R. Sun, and B. G. Shen

Institute of Physics, Beijing National Laboratory for Condensed Matter Physics and State Key Laboratory of Magnetism, Chinese Academy of Sciences, Beijing 100190, People's Republic of China

(Presented 7 November 2013; received 22 September 2013; accepted 29 October 2013; published online 29 January 2014)

The static and dynamic lattice strain effects on the competition between ferromagnetic and charge/orbital ordering (COO) phase, phase separation (PS) and transport properties were studied in $\text{Pr}_{0.7}(\text{Ca}_{0.6}\text{Sr}_{0.4})_{0.3}\text{MnO}_3$ (PCSMO) films. It is found that the tensile strained films show pronounced percolative transport behaviors with increased hysteresis, indicating that the stability of the long-range COO is enhanced by the tensile strain. On the other hand, a nearly reversible insulator-metal transition was observed in the compressive strained films, suggesting a strong suppression of the long-range COO. The experiment of dynamic strain effect induced by the bias electric field further verifies the conclusion. Moreover, coactions of the ferroelectric polarization of the substrate and the dynamic strain effect on the PS were found in present PCSMO/PMN-PT film. © 2014 AIP Publishing LLC. [<http://dx.doi.org/10.1063/1.4863383>]

Perovskite manganites $\text{R}_{1-x}\text{A}_x\text{MnO}_3$ (R and A being trivalent and divalent cations) have been extensively studied in recent years due to the coexistence of coupled charge, spin, lattice, and orbital degrees of freedom.¹ As well known, the average radius of R^{3+} and A^{2+} determine the band of the perovskite manganites, which could adjust the tilting of the MnO_6 octahedra, resulting in many intriguing phenomena, such as charge/orbital ordering (COO), phase separation (PS), and metal-insulator transition. $\text{Pr}_{1-x}\text{Ca}_x\text{MnO}_3$ system with $0.3 \leq x < 0.75$ has a narrow one-electron bandwidth of e_g band (W) and exhibits COO.² To introduce chemical pressure by substitute Sr^{2+} for Ca^{2+} would modify the local structural parameters such as Mn-O-Mn bond angle and bond length, thereby widen the e_g band.² As a result, the coexistence and competition of the COO phase with a ferromagnetic (FM) metallic phase emerges upon Sr doping, and an insulator-metal transition (IMT) appears in a percolative manner or via linking of the separated ferromagnetic clusters.^{2,3} On the other hand, the lattice strain, induced by either the lattice mismatch between the bulk and substrate or a bias field on the ferroelectric substrate, plays an important role in controlling the magnetic and transport properties of films with PS character.⁴⁻⁸ It can influence the subtle balance of free energy between the coexistent COO and FM phases by modifying MnO_6 octahedron distortion and thus the strength of the double exchange interaction and the Jahn-Teller (JT) electron-lattice coupling.⁶⁻⁸ In this paper, we report the influence of static and dynamic lattice strain effects on the competition between FM and COO phase, PS and the transport properties in $\text{Pr}_{0.7}(\text{Ca}_{0.6}\text{Sr}_{0.4})_{0.3}\text{MnO}_3$ (PCSMO) films. Four kinds of (001) single crystals with different lattice constant, LaAlO_3 (LAO)(3.788 Å), LSAT(3.868 Å), NdGaO_3 (NGO)

(3.853 Å), and PMN-PT(4.017 Å), are chosen as substrates to introduce various lattice strains in the films. Meanwhile, the dynamic lattice strain effect is studied in the film on PMN-PT, taking advantage of the excellent inverse piezoelectric character of PMN-PT substrate.^{5,7,8}

The PCSMO films were fabricated by pulsed laser deposition (PLD), a KrF excimer laser (248 nm) with a pulsed energy of 300 mJ and a repetition of 1 Hz was used. The temperature of the substrate was kept at 700 °C and the oxygen pressure at 0.67 mTorr during the deposition. After the deposition, the samples were cooled to room temperature in a pure oxygen atmosphere of 1 atm. The thickness of the films was controlled to be 30 nm. The magnetization and transport properties were measured using a superconducting quantum interference device (SQUID)–Vibrating Sample Magnetometer (VSM).

X ray diffraction (XRD) using $\text{Cu-K}\alpha$ radiation was carried out at room temperature to identify the structure of PCSMO bulk and films. It is found that the bulk crystallizes in orthometric structure with space group of Pnma, and the pseudocubic lattice parameters are determined to be 3.854 Å ($a = 5.462$ Å, $b = 5.449$ Å, $c = 7.709$ Å). All the films are highly oriented along the [001] direction and no other impurity phases are found. Typically, Fig. 1 shows a θ - 2θ XRD pattern for the 30 nm PCSMO film on PMNPT substrate. One can find that the reflections from the film separate from those of PMNPT substrate, indicating a strain induced by substrate owing to the mismatch between them. The out-of-plane lattice parameter c for 30 nm PCSMO/PMN-PT film is determined to be 3.815 Å, and the out-of-plane strain is correspondingly -1.01% by using $\varepsilon_{zz} = (c_{\text{film}} - c_{\text{bulk}})/c_{\text{bulk}}$, indicating the film undergo compressive strain along the out-of-plane direction. Meanwhile, the corresponding in-plane strain is calculated as 0.73% by Poisson relation $\varepsilon_{xx} = -2\nu/(1 - \nu)\varepsilon_{zz}$ using $\nu = 0.4$.⁹ For the PCSMO/LSAT film, the c axis lattice parameter is 3.823 Å, undergoing an out-of-plane compressive strain

^{a)}Authors to whom correspondence should be addressed. Electronic addresses: wangjing@iphy.ac.cn and fxhu@iphy.ac.cn.

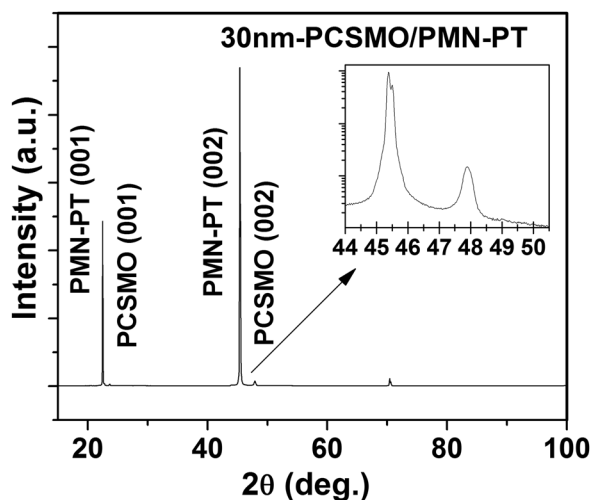


FIG. 1. X-ray diffraction patterns of the 30 nm PCSMO/PMN-PT films. The inset displays the corresponding details around the (002) peak.

($\varepsilon_{zz} = -0.82\%$) and an in-plane tensile strain ($\varepsilon_{xx} = 0.59\%$). The full information of all films' lattice parameter and lattice strain are listed in Table I. On the other hand, we found that the films on LAO and NGO undergo out-of-plane tensile strains (1.61% for the film on LAO, 0.37% for the one on NGO) and in-plane compressive strains (-1.16% for the former, and -0.26% for the latter). The introduced different tensile and compressive strain would impose different effects on the competition and the subtle balance between FM and CO phases.

Figure 2 displays the temperature dependence of resistance (R - T) for bulk. The inset plots the temperature dependent magnetization measured under 0.01 T using zero-field cooling (ZFC) and field cooling (FC). One could find that a long range ferromagnetic ordering appears at low temperature, and the Curie temperature is about 150 K. A separation between the FC and ZFC curves appears below the transition temperature, indicating spin glass type behaviors caused by the gradual block of the moments of the ferromagnetic clusters with decreasing temperature.⁴ The RT curve shows an IMT with an obvious thermal hysteresis (~ 3.5 K) around 173 K between the cooling and the warming processes, which indicates the coexistence of the COO insulating and FM metallic phases at low temperature.^{2,3} Upon the strong competition between the COO and the metallic ferromagnetism, a phase separation appears. With temperature decreases, the FM fractions develop and reach the percolation threshold, resulting in the IMT with thermal hysteresis.³

Figure 3 shows a comparison of the temperature dependent normalized resistance (R) for the PCSMO bulk and 30 nm

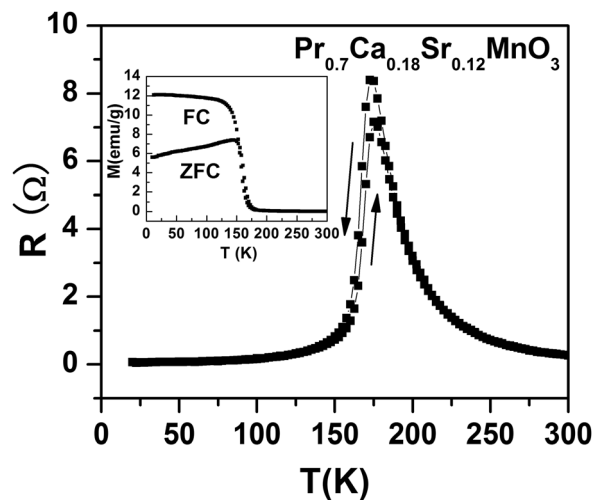


FIG. 2. Temperature dependence of the resistance for PCSMO bulk. The inset shows temperature dependent ZFC and FC magnetization under 0.01 T.

films on different substrates. It is found that the transition temperature of the 30 nm film on LSAT decreases by ~ 43 K with the hysteresis gap broadening from 3.5 K (bulk value) to 8.5 K. While for the one on PMN-PT with a larger in-plane tensile strain, a substantial reduction in the transition temperature (~ 84 K) and a pronounced hysteresis gap (~ 20 K) are observed. This result demonstrates that the in-plane tensile strain (out-of-plane compressive strain) can enhance the stabilities of the long-range COO phases and increase the characteristic of phase separation, and a larger tensile strain leads to a more strong effect. It is known that the relative stabilities of the COO and FM metal states are decided by the effective one-electron bandwidth of the e_g electron at the Mn^{3+} sites (W).^{2,4} The in-plane tensile strain could compress the MnO_6 octahedrons in out-of-plane direction and intensify the distortion of MnO_6 , leading to an enhancement of the collective JT distortion and a reduction of W . Consequently, the long range COO state is favored, resulting in the widening of the hysteresis gap and the shift of the transition point towards low temperature.

On the other hand, the films under in-plane compressive strain (on NGO and LAO) show different behaviors. Fig. 3(b) shows the comparison of the temperature dependent normalized resistance between in-plane compressive strained films and the bulk. We can find that hysteresis gap around the IMT becomes trivial for the films. It is only 1.3 K and 0.1 K for the films on NGO and LAO, respectively, implying that long-range COO is strongly suppressed by in-plane compressive strain and the percolative manner no longer dominates the transport behavior around the IMT. Actually, the

TABLE I. Summary of substrate and PCSMO film properties, c-axis lattice constant, out-plane and in-plane strain.

Substrate	Lattice constant of substrate (\AA)	Lattice constant of bulk (\AA)	c-axis lattice constant (\AA)	Out-plane strain (%)	In-plane strain (%)
LaAlO ₃	3.788	3.854	3.917	1.61	-1.16
NdGaO ₃	3.853		3.869	0.37	-0.26
LSAT	3.868		3.823	-0.82	0.59
PMNPT	4.017		3.815	-1.01	0.73

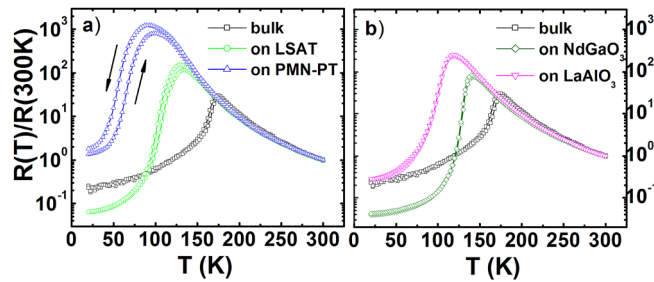


FIG. 3. The dependence of normalized resistivity on temperature for (a) tensile strained films (PCSMO/LSAT, PCSMO/PMN-PT) and (b) compressive strained films (PCSMO/LaAlO₃, PCSMO/NdGaO₃) compared to the bulk.

compressive strain would decrease the Mn-O-Mn bond length and increase the in-plane transfer integral for the e_g orbital electron hopping, thereby enhance the long range FM phase. In this case, the metal conductivity, as well as IMT should be mostly dominated by double-exchange interaction as general.

Considering that introducing static strain using different substrates may introduce other unexpected factors such as defects, microstructure, compositions deviation in parallel, we further investigated the dynamic strain effect in films of 30 nm-PCSMO/PMN-PT taking advantage of the excellent inverse piezoelectric character of PMN-PT. Figures 4(a) and 4(b) display the temperature dependence of resistance $R(T)$ for the 30 nm PCSMO/PMN-PT film under bias fields of +8 kV/cm and -8 kV/cm compared to zero, respectively. For the case of applying positive bias, the resistance of the film in the cooling process reduces $\sim 56\%$ at the IMT temperature of 90 K. Meanwhile the thermal hysteresis decreases from 20 K to 6 K and the IMT temperature increases from ~ 90 K to 107 K (determined from the cooling process, see Fig. 4(a)), implying that the COO state is suppressed and the long-range FM phase enhances. Previous researches have shown that the bias field could induce an in-plane contraction strain ($\sim -0.06\%$ for 8 kV/cm) in (001)-PMN-PT due to the converse piezoelectric effect,¹⁰ which could transfer to the film and reduce its in-plane tensile strain.¹¹ Thus, the reduction of the in-plane tensile strain will push the balance between FM and COO phases towards the former through release the Jahn-Teller distortion, consistent with the results of the static lattice strain effect shown in Fig. 3(a). This fact further verifies that the tensile strain favors the long-range COO.

Much to our surprise, with a negative bias field applied, the resistance increases by $\sim 82\%$ at the transition point of ~ 98 K in the warming process and decreases by $\sim 40\%$ at $T_{IM} = \sim 90$ K in the cooling process (see Fig. 4(b)). Note that the resistance below the IMT temperature in the warming process turns to be larger than the one in the cooling process upon negative bias. This phenomenon is contrary to the percolative manner in the phase separated system where the

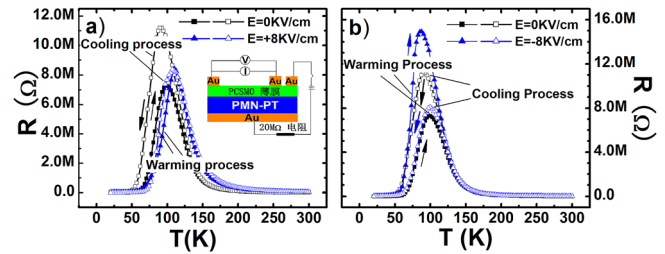


FIG. 4. The temperature dependence of the resistance for the 30 nm-PCSMO/PMN-PT film under a bias field of (a) +8 kV/cm and (b) -8 kV/cm in comparison with the one under 0 kV/cm. The inset of (a) shows a schematic diagram of the PCSMO/PMN-PT structure and the circuit for electrical measurements.

resistance at low temperature in the warming process is relative lower than the one in the cooling process due to the dominant long-range FM state at low temperature.^{3,12} This unexpected behavior could not be understood only in the framework of strain effect. Note that the bias field not only induces the piezoelectric effect but also poles the PMN-PT substrate.¹³ The bias field could induce charge accumulation of charge at the interface between insulating COO and metallic FM regions and move the interface, thereby changing the relative volume fraction of the COO and FM regions.¹³ Thus, the balance between two phases would be affected by the coactions of the polarization and strain effects as well as their competition. Meanwhile, one note that the resistance around the transition shows only a small increase in the warming process while a positive bias field was applied, suggesting the coactions and competition between the polarization and strain effect may behave different in different poling state. However, the detailed principle is still unclear at this moment. To completely understand the role of the bias field in affecting the PS and the competition between COO and FM phases, further investigations are still required.

This work was supported by National Basic Research of China (973 program, Grant Nos. 2012CB933000, 2011CB921801, and 2014CB643702), and the National Natural Science Foundation of China (Grant Nos. 11174345, 11074286 and 51271196).

¹J. M. D. Coey *et al.*, *Adv. Phys.* **58**, 571 (2009).

²Y. Tomioka and Y. Tokura, *Phys. Rev. B* **66**, 104416 (2002).

³M. Uehara *et al.*, *Nature* **399**, 560 (1999).

⁴R. C. Budhani *et al.*, *Phys. Rev. B* **65**, 014429 (2001).

⁵R. K. Zheng *et al.*, *Phys. Rev. B* **75**, 024110 (2007).

⁶J. Zhang *et al.*, *Phys. Rev. B* **64**, 184404 (2001).

⁷J. Wang *et al.*, *Appl. Phys. Lett.* **96**, 052501 (2010).

⁸K. Dörr *et al.*, *Eur. Phys. J. B* **71**, 361 (2009).

⁹L. Ranno *et al.*, *Appl. Surf. Sci.* **188**, 170 (2002).

¹⁰C. Thiele *et al.*, *Phys. Rev. B* **75**, 054408 (2007).

¹¹M. D. Biegalski *et al.*, *Appl. Phys. Lett.* **96**, 151905 (2010).

¹²T. Z. Ward *et al.*, *Nat. Phys.* **5**, 885 (2009).

¹³T. Wu *et al.*, *Phys. Rev. Lett.* **86**, 5998 (2001).